Research Article

Muhammad Farooq, Zia Ullah, Muhammad Zeb, Hijaz Ahmad, Muhammad Ayaz, Muhammad Sulaiman, Chutarat Tearnbucha*, and Weerawat Sudsutad

Homotopy analysis method with application to thin-film flow of couple stress fluid through a vertical cylinder

https://doi.org/10.1515/phys-2022-0056
received November 07, 2021; accepted March 20, 2022

Abstract: This work solves the problem of thin-film withdrawal and drainage of a steady incompressible couple stress fluid on the outer surface of a vertical cylinder. The governing equations for velocity and temperature distributions are subjected to the boundary conditions and solved with the help of homotopy analysis method. The obtained expressions for flow profile, temperature profile, average velocity, volume flow rate, and shear stress confirmed that the thin-film flow of couple stress fluid highly depends on involved parameters say Stokes number S_t, vorticity parameter λ, couple stress parameter η, and Brinkman number Br presented in the graphical description as well.

Keywords: thin film flow, withdrawal, drainage, couple stress fluid, vertical cylinder, differential equations, homotopy analysis method

*** Corresponding author: Chutarat Tearnbucha,** Department of General Education, Faculty of Science and Health Technology, Navamindradhiraj University, Bangkok, 10300 Thailand, e-mail: chutaratt@nmu.ac.th
Muhammad Farooq, Zia Ullah: Department of Mathematics, Abdul Wali Khan University, Mardan, Khyber Pakhtunkhwa, Pakistan
Muhammad Zeb: Department of Mathematics, COMSATS University Islamabad, Attock Campus, Punjab, Pakistan
Hijaz Ahmad: Section of Mathematics, International Telematic University Uninettuno, Corso Vittorio Emanuele II, 39, 00186 Roma, Italy, e-mail: hijaz555@gmail.com
Muhammad Ayaz, Muhammad Sulaiman: School of Science, Xi'an University of Architecture and Technology, Xi'an 710055, China
Weerawat Sudsutad: Department of Statistics, Faculty of Science, Ramkhamhaeng University, Bangkok, 10240 Thailand

1 Introduction

Non-Newtonian fluids have a vigorous place in the present research due their prevalent importance in the food, chemical, construction, pharmaceutical industries *etc*. Non-Newtonian fluids cover production of synthetic items, all types of automobiles, food products, biotic fluids, cable and filament layer, sheets manufacturing, denitrification freezing, gassy flow, penetrating sludge, heat up tubes, *etc*.

All non-Newtonian fluids are not of the same kind, so for better understanding different types of non-Newtonian fluids, these fluids are categories in different fluid models such as differential type and rate type fluids models. Couple stress fluid is one among these fluids and its equation is centered on solid theoretic grounds, whenever relationship among stress and strain are not linear. The behavior of couple stress fluid has been studied in many research works which have come up with fruitful results. The couple stress fluids model introduced by Stokes [1], has distinct characteristics, such as the presence of couple stresses, non-symmetric stress tensor and body couples. Many scholars have scrutinized the flow behavior of couple stress fluid, like Devakar *et al.* [2] studied the couple stress fluid with slip boundary conditions in parallel plates. Jangili *et al.* [3] have demonstrated the irreversibility rate for the couple stress fluid under the effect of variable viscosity and thermal conductivity. Farooq *et al.* [4] have investigated the behavior of couple stress fluid with temperature dependent variable viscosity on inclined plate. The importance of this theory is consideration of the rotational effects, which is not considered in Navier–Stokes equations. Applications of couple stress fluids are in industries such as extrusion for polymer fluids, colloidal solution, and the lubrication of engine and bearings [5]. Its applications in biomechanics are discussed in refs [6–8].

Several researchers have studied and addressed the physical relevance of thin film. Miladinova *et al.* [9] described, for example, the thin film power law model fluid flowing on a tilted plate and found a nonlinear interaction saturation observed with permanent wave of finite amplitude. Alam *et al.* [10] studied Johnson–Segalman thin film flow for lifting and drainage on a vertical surface and have discussed the effects of involved parameters on film flow. Shah *et al.* [11] presented the film flow of second grade in a straight annular die and developed the governing equations to analyze the process of wire coating. The magnetohydrodynamics (MHD) boundary layer flow of mass and heat transfer marvels with radiation and dissipative impacts past a permeable stretchable surface was explored by Kar *et al.* [12]. Moreover, Nayak *et al.* [13] have presented heat and mass transfer phenomenon in the boundary layer flow of electrically conducting viscoelastic fluid in the presence of source/sink, chemical reaction, and normal magnetic field, and found that magnetic field is very useful in promoting the velocity and concentration distribution. Also, the investigation shows that the expanding upsides of the heat source boundary and the shortfall of the permeable boundary upgrade the stream nearby the plate. In ref. [14], Gowda *et al.* have presented heat and mass transfer briefly in ferromagnetic fluid on the surface of a stretchable sheet. Gul *et al.* [15] have studied third grade fluid thin film flow for lifting and drainage with the impact of MHD and heat subordinate thickness. On the other hand, Ahmad *et al.* [16] investigated the unsteady free convection flow of a second grade fluid.

Siddiqui *et al.* [17] have studied the flow of thin films of third- and fourth-grade fluids falling on an inclined plane and vertical cylinder *via* homotopy analysis method (HAM). Farooq *et al.* [18,19] investigated the withdrawal and drainage of generalized second-grade fluid with and without slip conditions on a vertical cylinder. The literature review shows that approximate analytical techniques [20–40] are very strong tools to solve highly nonlinear differential equations, and one among these is HAM [41]. In this work we have solved the problem of thin film flow of couple stress fluid on the outer surface of vertical cylinder, and the developed mathematical model is analyzed with the help of HAM.

2 Lifting problem

Consider incompressible, non-isothermal couple stress fluid in a container, and a vertical cylinder passing through the container, moving upward contacting fluid from the container, develops a thin film of constant thickness δ of the fluid on the outer surface symmetrically. The cylindrical coordinates are fixed as the axial axis is located at the center of the cylinder and the radial axis is kept along the radius R of the cylinder as shown in Figure 1(a). Assuming that the flow is steady and has no change with respect to θ the velocity and temperature fields are:

$$V = [0, 0, w(r)], \quad \theta = \theta(r). \tag{1}$$

The following are the basic equations that regulate the flow of an incompressible non-isothermal couple stress fluid:

$$\nabla \cdot V = 0, \tag{2}$$

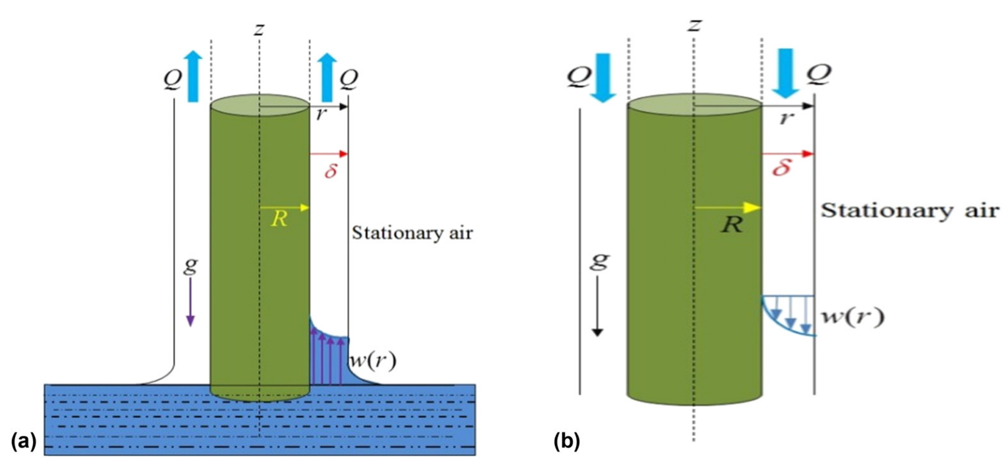

Figure 1: (a) Geometry of the lifting problem. (b) Geometry of the drainage.

$$\rho \frac{d\boldsymbol{V}}{dt} = \rho \boldsymbol{f} - \nabla p + \nabla \cdot \boldsymbol{T} - \eta \nabla^4 \boldsymbol{V}, \tag{3}$$

$$\rho C_p \frac{d\theta}{dt} = k\nabla^2\theta + \mathrm{trc}(\boldsymbol{T} \cdot \boldsymbol{L}), \tag{4}$$

where $\mathbf{V}$ represents the velocity vector and $\frac{d}{dt}$ is material time derivative defined as

$$\frac{d}{dt}(\cdot) = \left(\frac{\partial}{\partial t} + V \cdot \nabla\right)(\cdot), \tag{5}$$

k is the thermal conductivity, ρ is the constant density, C_p is the specific heat constant, f is the body force, θ is the temperature, p is the dynamic pressure, and T is the stress tensor taken as:

$$T = \mu A_1, \tag{6}$$

where μ is the viscosity of the fluid, and A_1 is the first Rivlin–Erickson tensor.

$$A_1 = L + L^T, \text{ and } L = \nabla V. \tag{7}$$

The velocity field (1), balances Eq. (2), and reduces Eq. (3), in the following components:
r-component:

$$\frac{\partial p}{\partial r} = 0. \tag{8}$$

θ-component:

$$\frac{1}{r}\frac{\partial p}{\partial \theta} = 0, \tag{9}$$

z-component:

$$\begin{aligned} \frac{\partial p}{\partial z} &= -\rho g + \mu \frac{1}{r}\frac{d}{dr}\left[r\frac{dw}{dr}\right] \\ &- \eta\left[\frac{1}{r}\frac{d}{dr}\left(r\frac{d}{dr}\right)\right]\left[\frac{1}{r}\frac{d}{dr}\left(r\frac{dw}{dr}\right)\right]. \end{aligned} \tag{10}$$

Using Eqs. (8) and (9), Eq. (10) becomes

$$\begin{aligned} \frac{dp}{dz} &= -\rho g + \mu \frac{1}{r}\frac{d}{dr}\left[r\frac{dw}{dr}\right] \\ &- \eta\left[\frac{1}{r}\frac{d}{dr}\left(r\frac{d}{dr}\right)\right]\left[\frac{1}{r}\frac{d}{dr}\left(r\frac{dw}{dr}\right)\right]. \end{aligned} \tag{11}$$

Consider that the pressure is atmospheric, then $\frac{dp}{dz} = 0$, and so Eq. (11) gets the form:

$$\begin{aligned} &\frac{d^4w}{dr^4} + \frac{2}{r}\frac{d^3w}{dr^3} + \left(\frac{1}{r^2} - \frac{\mu}{\eta}\right)\frac{d^2w}{dr^2} \\ &+ \left(\frac{1}{r^3} - \frac{\mu}{\eta r}\right)\frac{dw}{dr} = -\frac{\rho g}{\eta}. \end{aligned} \tag{12}$$

The velocity and temperature fields simplify Eq. (4) as:

$$\kappa\left(\frac{d^2\theta}{dr^2} + \frac{1}{r}\frac{d\theta}{dr}\right) + \mu\left(\frac{dw}{dr}\right)^2 = 0. \tag{13}$$

For the fourth order (12) and second order (13) nonlinear differential equations, the following boundary conditions can be set from the geometry as given:

$$\begin{aligned} &w = U, \quad \frac{d^2w}{dr^2} = 0, \quad \theta = \theta_0 \quad \text{at } r = R, \\ &\frac{dw}{dr} = 0, \quad \frac{d^3w}{dr^3} = 0, \quad \frac{d\theta}{dr} = 0 \quad \text{at } r = R + \delta. \end{aligned} \tag{14}$$

Using the non-dimensional parameters

$$\begin{aligned} &w^* = \frac{w}{U}, \ r^* = \frac{r}{\delta}, \ \lambda = \frac{\mu\delta^2}{\eta}, \ S_t = \frac{\rho g \delta^2}{\mu U}, \\ &\mathrm{Br} = \frac{\mu_{\mathrm{eff}} U^2}{(\theta_1 - \theta_0)k}, \ R^* = \frac{R}{\delta}. \end{aligned} \tag{15}$$

After dropping asterisks Eqs. (12–14) become

$$\begin{aligned} &\frac{d^4w}{dr^4} + \frac{2}{r}\frac{d^3w}{dr^3} + \left(\frac{1}{r^2} - \lambda\right)\frac{d^2w}{dr^2} + \left(\frac{1}{r^3} - \frac{\lambda}{r}\right)\frac{dw}{dr} \\ &= -\lambda S_t, \end{aligned} \tag{16}$$

$$\left(\frac{d^2\theta}{dr^2} + \frac{1}{r}\frac{d\theta}{dr}\right) + \frac{\mu U^2}{\kappa(\theta_1 - \theta_0)}\left(\frac{dw}{dr}\right)^2 = 0. \tag{17}$$

Using the previously defined dimensionless quantities, Eq. (17) becomes

$$\left(\frac{d^2\theta}{dr^2} + \frac{1}{r}\frac{d\theta}{dr}\right) + \mathrm{Br}\left(\frac{dw}{dr}\right)^2 = 0. \tag{18}$$

The dimensionless form of the boundary conditions given in (14) take the form:

$$\begin{aligned} &w = 1, \quad \frac{d^2w}{dr^2} = 0, \ \theta = \theta_0 \quad \text{at } r = R, \\ &\frac{dw}{dr} = 0, \ \frac{d^3w}{dr^3} = 0, \quad \frac{d\theta}{dr} = 0 \quad \text{at } r = R + 1. \end{aligned} \tag{19}$$

3 Solution of lifting problem using HAM

The approximate analytical technique, HAM, is used to solve Eqs. (16) and (18), together with Eq. (19). Fundamental roots of the model equations *via* HAM are given below in detail.

$$L_{\widehat{w}}(\widehat{w}) = w^{iv}, L_{\widehat{\theta}}(\theta) = \theta'', \tag{20}$$

linear operators $L_{\widehat{w}}$ are signified as

$$L_{\widehat{w}}((e^{2R} - e^{2\delta})(e^{2\delta}e^{-r} + e^{r})) = 0,\quad L_{\widehat{\theta}}(e^{2R} + e^{2\delta}e^{r}) = 0. \tag{21}$$

The consistent non-linear operators are reasonably selected as $N_{\widehat{w}}$ and $N_{\widehat{\theta}}$, and recognized in system as:

$$N_{\widehat{w}}[\widehat{w}(r;\zeta)] = [\widehat{w}]_{rrrr} + \frac{2}{r}[\widehat{w}]_{rrr} + \left(\frac{1}{r^2} - \lambda\right)[\widehat{w}]_{rr} + \left(\frac{1}{r^3} - \frac{\lambda}{r}\right)[\widehat{w}]_{r} + \lambda S_t, \tag{22}$$

$$N_{\widehat{\theta}}[\widehat{w}(r;\zeta), \widehat{\theta}(r;\zeta)] = [\widehat{\theta}]_{rr} + \frac{1}{r}[\widehat{\theta}]_{r} + \mathrm{Br}[\widehat{w}_r]^2. \tag{23}$$

For Eqs. (20) and (21), the 0th-order system can be written as:

$$(1-\zeta)L_{\widehat{w}}[\widehat{w}(r;\zeta) - \widehat{w}_0(r)] = p\hbar_{\widehat{w}}N_{\widehat{w}}[\widehat{w}(r;\zeta)], \tag{24}$$

$$(1-\zeta)L_{\widehat{\theta}}[\widehat{\theta}(r;\zeta) - \widehat{\theta}_0(r)] = p\hbar_{\widehat{\theta}}N_{\widehat{\theta}}[\widehat{w}(r;\zeta), \widehat{\theta}(r;\zeta)]. \tag{25}$$

While BCs are:

$$\widehat{w}(r;\zeta)|_{r=0} = 1,\ \left.\frac{d^2\widehat{w}(r;\zeta)}{dr^2}\right|_{r=0} = 0,$$
$$\widehat{\theta}(r;\zeta)|_{r=0} = \widehat{\theta}_0(r;\zeta)|_{r=0} \tag{26}$$
$$\left.\frac{d\widehat{w}(r;\zeta)}{dr}\right|_{r=1} = 0,\ \left.\frac{d^3\widehat{w}(r;\zeta)}{dr^3}\right|_{r=1} = 0,\ \left.\frac{d\widehat{\theta}(r;\zeta)}{dr}\right|_{r=1} = 0.$$

Here ζ is the embedding parameter $\zeta \in [0, 1]$, to regulate for the solution convergence of $\hbar_{\widehat{w}}, \hbar_{\widehat{\theta}}$ is used. When $\zeta = 0$ and $\zeta = 1$ we have:

$$\widehat{w}(r;1) = \widehat{w}(r), \tag{27}$$

$$\widehat{\theta}(r;1) = \widehat{\theta}(r), \tag{28}$$

Expand the $\widehat{w}(r;\zeta), \widehat{\theta}(r;\zeta)$ through Taylor's series for $\zeta = 0$

$$\widehat{w}(r;\zeta) = \widehat{w}_0(r) + \sum_{n=1}^{\infty}\widehat{w}_n(r)\zeta^n,\quad \widehat{\theta}(r;\zeta) = \widehat{\theta}_0(r) + \sum_{n=1}^{\infty}\widehat{\theta}_n(r)\zeta^n. \tag{29}$$

$$\widehat{w}_n(r) = \frac{1}{n!}\left.\frac{\partial\widehat{w}(r;\zeta)}{\partial r}\right|_{p=0},\ \widehat{\theta}_n(r) = \frac{1}{n!}\left.\frac{\partial\widehat{\theta}(r;\zeta)}{\partial r}\right|_{p=0}. \tag{30}$$

While BCs are:

$$\widehat{w}(0) = 1,\quad \widehat{w}''(0) = 0,\quad \widehat{\theta}(0) = \widehat{\theta}_0(0)$$
$$\widehat{w}'(\delta) = 0,\quad \widehat{w}'''(\delta) = 0,\quad \widehat{\theta}'(\delta) = 0. \tag{31}$$

Now

$$\mathfrak{R}_n^{\widehat{w}}(r) = [\widehat{w}]_{n-1}^{\mathrm{iv}} + \frac{2}{r}[\widehat{w}''']_{n-1} + \left(\frac{1}{r^2} - \lambda\right)[\widehat{w}'']_{n-1} + \left(\frac{1}{r^3} - \frac{\lambda}{r}\right)[\widehat{w}']_{n-1} + \lambda S_t, \tag{32}$$

$$\mathfrak{R}_n^{\widehat{\theta}}(r) = [\widehat{\theta}'']_{n-1} + \frac{1}{r}[\widehat{\theta}']_{n-1} + \mathrm{Br}[\widehat{w}'']_{n-1}^2, \tag{33}$$

and $\chi_n = \begin{cases} 0, & \text{if } n \le 1, \\ 1, & \text{if } n > 1. \end{cases}$

4 Drainage problem

Consider incompressible, non-isothermal couple stress fluid in a container, and a vertical cylinder, moving downward contacting the fluid from the container, develops a thin film of constant thickness δ of the fluid on the outer surface symmetrically. The cylindrical coordinates are fixed as the axial axis is located at the center of the cylinder and the radial axis is kept along the radius R of the cylinder as shown in Figure 1(b). Assuming that the flow is steady and has no change with respect to θ, the velocity field and temperature distribution are:

$$V = [0, 0, w(r)],\ \theta = \theta(r). \tag{34}$$

For the drainage problem, we take the dimensionless form of the governing equations after using dimensionless parameters given in Eq. (15) as under:

$$\frac{d^4w}{dr^4} + \frac{2}{r}\frac{d^3w}{dr^3} + \left(\frac{1}{r^2} - \lambda\right)\frac{d^2w}{dr^2} + \left(\frac{1}{r^3} - \frac{\lambda}{r}\right)\frac{dw}{dr} = \lambda S_t, \tag{35}$$

$$\left(\frac{d^2\theta}{dr^2} + \frac{1}{r}\frac{d\theta}{dr}\right) + \mathrm{Br}\left(\frac{dw}{dr}\right)^2 = 0, \tag{36}$$

the boundary conditions are:

$$w = 0,\quad \frac{d^2w}{dr^2} = 0,\ \theta = \theta_0 \quad \text{at} \quad r = R,$$
$$\frac{dw}{dr} = 0,\ \frac{d^3w}{dr^3} = 0,\ \frac{d\theta}{dr} = 0 \quad \text{at} \quad r = R + 1. \tag{37}$$

5 Solution of drainage problem using HAM

The approximate analytical technique, HAM, is used to solve Eqs. (35) and (36), together with Eq. (37). Fundamental roots of the model equations *via* HAM are given below in detail:

$$L_{\widehat{w}}(\widehat{w}) = w^{\mathrm{iv}},\ L_{\widehat{\theta}}(\theta) = \theta''. \tag{38}$$

Linear operators $L_{\widehat{w}}$ are signified as

$$L_{\widehat{w}}((e^{2R} - e^{2\delta})(e^{2\delta}e^{-r} + e^{r})) = 0, \quad L_{\widehat{\theta}}(e^{2R} + e^{2\delta}e^{r}) = 0. \tag{39}$$

The consistent nonlinear operators are reasonably selected as $N_{\widehat{w}}$ and $N_{\widehat{\theta}}$, and recognize in system as:

$$N_{\widehat{w}}[\widehat{w}(r;\zeta)] = [\widehat{w}]_{rrrr} + \frac{2}{r}[\widehat{w}]_{rrr} + \left(\frac{1}{r^2} - \lambda\right)[\widehat{w}]_{rr} + \left(\frac{1}{r^3} - \frac{\lambda}{r}\right)[\widehat{w}]_{r} - \lambda \mathrm{S}_{\mathrm{t}}, \tag{40}$$

$$N_{\widehat{\theta}}[\widehat{w}(r;\zeta), \widehat{\theta}(r;\zeta)] = [\widehat{\theta}]_{rr} + \frac{1}{r}[\widehat{\theta}]_{r} + \mathrm{Br}[\widehat{w}_r]^2.$$

For Eq. (39), the 0th-order system is written as

$$(1 - \zeta)L_{\widehat{w}}[\widehat{w}(r;\zeta) - \widehat{w}_0(r)] = p\hbar_{\widehat{w}}N_{\widehat{w}}[\widehat{w}(r;\zeta)], \quad (1 - \zeta)L_{\widehat{\theta}}[\widehat{\theta}(r;\zeta) - \widehat{\theta}_0(r)] = p\hbar_{\widehat{\theta}}N_{\widehat{\theta}}[\widehat{w}(r;\zeta), \widehat{\theta}(r;\zeta)]. \tag{41}$$

While BCs are:

$$\widehat{w}(r;\zeta)|_{r=0} = 1, \quad \left.\frac{d^2\widehat{w}(r;\zeta)}{dr^2}\right|_{r=0} = 0, \quad \widehat{\theta}(r;\zeta)|_{r=0} = \widehat{\theta}_0(r;\zeta)|_{r=0}, \quad \left.\frac{\mathrm{d}\widehat{w}(r;\zeta)}{\mathrm{d}r}\right|_{r=1} = 0, \quad \left.\frac{\mathrm{d}^3\widehat{w}(r;\zeta)}{\mathrm{d}r^3}\right|_{r=1} = 0, \quad \left.\frac{\mathrm{d}\widehat{\theta}(r;\zeta)}{\mathrm{d}r}\right|_{r=1} = 0. \tag{42}$$

Here ζ is the embedding parameter $\zeta \in [0, 1]$, to regulate for the solution convergence of $\hbar_{\widehat{w}}$, $\hbar_{\widehat{\theta}}$ is used. When $\zeta = 0$ and $\zeta = 1$ we have:

$$\widehat{w}(r;1) = \widehat{w}(r), \tag{43}$$

$$\widehat{\theta}(r;1) = \widehat{\theta}(r). \tag{44}$$

Expand the $\widehat{w}(r;\zeta)$, $\widehat{\theta}(r;\zeta)$ through Taylor's series for $\zeta = 0$

$$\widehat{w}(r;\zeta) = \widehat{w}_0(r) + \sum_{n=1}^{\infty}\widehat{w}_n(r)\zeta^n, \quad \widehat{\theta}(r;\zeta) = \widehat{\theta}_0(r) + \sum_{n=1}^{\infty}\widehat{\theta}_n(r)\zeta^n, \tag{45}$$

$$\widehat{w}_n(r) = \frac{1}{n!}\left.\frac{\partial\widehat{w}(r;\zeta)}{\partial r}\right|_{p=0}, \quad \widehat{\theta}_n(r) = \frac{1}{n!}\left.\frac{\partial\widehat{\theta}(r;\zeta)}{\partial r}\right|_{p=0}. \tag{46}$$

While BCs are:

$$\widehat{w}(0) = 1, \quad \widehat{w}''(0) = 0, \quad \widehat{\theta}(0) = \widehat{\theta}_0(0), \quad \widehat{w}'(\delta) = 0, \quad \widehat{w}'''(\delta) = 0, \quad \widehat{\theta}'(\delta) = 0. \tag{47}$$

Now

$$\mathfrak{R}_n^{\widehat{w}}(r) = [\widehat{w}]_{n-1}^{\mathrm{iv}} + \frac{2}{r}[\widehat{w}''']_{n-1} + \left(\frac{1}{r^2} - \lambda\right)[\widehat{w}'']_{n-1} + \left(\frac{1}{r^3} - \frac{\lambda}{r}\right)[\widehat{w}']_{n-1} - \lambda S_t, \tag{48}$$

$$\mathfrak{R}_n^{\widehat{\theta}}(r) = [\widehat{\theta}'']_{n-1} + \frac{1}{r}[\widehat{\theta}']_{n-1} + B_r[\widehat{w}'']_{n-1}^2, \tag{49}$$

here

$$\chi_n = \begin{cases} 0, & \text{if } n \le 1 \\ 1, & \text{if } n > 1. \end{cases} \tag{50}$$

6 Results and discussion

In this work, we have analyzed the thin film flow cases of lifting (Figure 1a) and drainage (Figure 1b) of a steady, incompressible, non-isothermal couple stress fluid flow on the outer surface of a vertical cylinder. The problem formulation and modeling of phenomena gave nonlinear ordinary differential equations. Due to nonlinearity, exact solutions of the problems seem to be difficult so an analytical technique, HAM, is used to obtain the required solutions. The behavior of the fluid to the involved parameter is studied with the help of tables and graphical representations.

6.1 Tabular description

Tables 1–4 are produced for different values of Stokes number, λ, Br, and η for the case of lifting. Tables 5–8 are produced for different values of Stokes number, λ, Br,

Table 1: Effect of S_t number on velocity profile $w(r)$, keeping $\lambda = 0.5$, Br = 0.7, $\eta = 0.8$

r	$S_t = 0.4$	$S_t = 0.7$	$S_t = 0.9$	$S_t = 1.1$
1	2.5359104	2.3195123	1.9303426	1.2283493
1.1	2.4875231	2.2174542	1.9158603	1.2093829
1.2	2.3919041	2.2046721	1.8660642	1.1836035
1.3	2.2570631	2.1031704	1.7318253	1.108333 6
1.4	1.8045716	2.0518034	1.6125352	1.0730631
1.5	1.9709216	1.7143519	1.5071462	0.9830613
1.6	1.7036087	1.5341518	1.4582441	0.9423721
1.7	1.5405933	1.5039821	1.2309302	0.9108622
1.8	1.4381075	1.3793046	1.1560128	0.8062925
1.9	1.3381075	1.2793046	1.0560128	0.7062925

Table 2: Effect of η on velocity profile $w(r)$, keeping $\lambda = 0.5$, Br = 0.7, $S_t = 0.4$

r	$\eta = 0.4$	$\eta = 0.5$	$\eta = 0.8$	$\eta = 0.9$
1	2.8548671	1.9494123	1.4383301	0.9572148
1.1	2.7187092	1.9272341	1.3365036	0.9237491
1.2	2.6710937	1.8191301	1.3030933	0.8335634
1.3	2.6010789	1.7519503	1.1103403	0.8112309
1.4	2.4510816	1.7312308	1.0387041	0.7038902
1.5	2.4170813	1.6403341	1.1933503	0.6201835
1.6	2.3497514	1.5135418	1.0380607	0.5325718
1.7	2.2083877	1.4186503	1.0097323	0.4578215
1.8	2.1541146	1.2049317	1.6730236	0.3618403
1.9	2.0686101	1.3857039	1.1545227	0.2179192

Table 3: Effect of λ on velocity profile $w(r)$, keeping $S_t = 0.6$, $\eta = 0.4$, Br = 0.7

r	$\lambda = 0.3$	$\lambda = 0.5$	$\lambda = 0.7$	$\lambda = 0.9$
1	1.974703 7	1.6864217	0.9674132	0.4516702
1.1	1.9473901	1.6253188	0.8524841	0.4134976
1.2	1.9230121	1.6048171	0.7345154	0.4081541
1.3	1.8834926	1.4756839	0.7044018	0.3810132
1.4	1.8716702	1.4537014	0.6547839	0.3711843
1.5	1.7520807	1.3924819	0.6291736	0.2781001
1.6	1.7201745	1.3453906	0.6171425	0.2501423
1.7	1.6536785	1.2601767	0.4186143	0.2012461
1.8	1.6453206	1.1843036	0.4451758	0.1965806
1.9	1.5274021	1.0158531	0.1646151	0.0410333

Table 4: Effect of Br on temperature distribution $\theta(r)$, where $S_t = 0.6$, $\eta = 0.4$, $\lambda = 0.7$

r	Br = 0.2	Br = 0.4	Br = 0.6	Br = 0.8
1	1.6504601	1.6435363	1.0635783	0.7835623
1.1	1.8261462	1.7257324	1.1285423	0.8238604
1.2	1.8363803	1.7381013	1.2071319	0.9021039
1.3	1.8445933	1.7636814	1.3536304	1.2839102
1.4	1.8937181	1.8734032	1.4157031	1.4040637
1.5	1.9908316	1.8917317	1.5317317	1.5209833
1.6	2.1785033	2.0156204	1.6156234	1.6241804
1.7	2.2390337	2.1039136	1.6534138	1.7053714
1.8	2.3797361	2.2685769	1.7673263	1.7235239
1.9	2.4903695	2.3790603	1.7732613	1.7713026

Table 5: Effect of S_t on velocity profile $w(r)$, keeping $\lambda = 0.5$, Br = 0.7, $\eta = 0.8$

r	$S_t = 0.4$	$S_t = 0.7$	$S_t = 0.9$	$S_t = 1.1$
1	0.4145093	1.6390924	2.4263639	2.6213414
1.1	0.5172042	1.7193835	2.5184721	2.721573 6
1.2	0.6523218	1.7475802	2.6069014	2.8145302
1.3	0.7113425	1.7670335	2.919463 7	3.0043533
1.4	0.8073451	1.7783413	2.9531423	3.1413732
1.5	0.8561582	1.8211802	2.9671814	3.3726331
1.6	0.9053348	1.8454321	2.9743103	3.4690103
1.7	1.9113507	1.9127422	2.9804937	3.5328372
1.8	1.9305286	2.1433426	2.9910495	3.5683403
1.9	1.97254703	2.2124862	2.9984973	3.573 8937

Table 6: Effect of η on velocity profile $w(r)$, keeping $\lambda = 0.5$, Br = 0.7, $S_t = 0.4$

r	$\eta = 0.4$	$\eta = 0.5$	$\eta = 0.8$	$\eta = 0.9$
1	0.8753037	0.5383921	0.0893624	0.0875105
1.1	0.8524853	0.5172315	0.0864305	0.0854136
1.2	0.8433541	0.5063602	0.0852642	0.0820248
1.3	0.8125602	0.4146318	0.0713532	0.0704109
1.4	0.8023367	0.4053431	0.0702823	0.0602573
1.5	0.6940716	0.5751134	0.3912141	0.0560248
1.6	0.5300337	0.3123405	0.2235173	0.0425613
1.7	0.5186526	0.2175421	0.1135137	0.0396518
1.8	0.4780402	0.3726403	0.1160152	0.0230457
1.9	0.4313723	0.2004273	0.1113046	0.0186237

Table 7: Effect of λ on velocity profile $w(r)$, where $S_t = 0.6$, $\eta = 0.4$, Br = 0.7

r	$\lambda = 0.3$	$\lambda = 0.5$	$\lambda = 0.7$	$\lambda = 0.9$
1	3.423840 5	2.3973714	1.8323324	0.9365204
1.1	3.3287324	2.1369601	1.7364732	0.8165125
1.2	3.1130282	2.0101581	1.7101322	0.7194276
1.3	3.0561301	1.5893402	1.6350164	0.6541441
1.4	2.6743152	1.5936538	1.6014932	0.4672452
1.5	2.6424101	1.6450571	1.4908379	0.4210752
1.6	2.5697234	1.6673909	1.4023246	0.3617614
1.7	2.5316782	1.6803621	1.3136239	0.3401589
1.8	2.4743341	1.7680219	1.1163218	0.3203567
1.9	2.3563132	1.8197368	1.0430135	0.2103675

and η for the case of drainage. The behavior of involved parameters on velocity profile and temperature distribution depicted in the tables is discussed thoroughly.

Table 1 shows the effects of Stokes number on the velocity profile during lifting, it is observed that increase in the value of Stokes number slows down the velocity profile.

Table 2, gives the effects of η on the velocity profile during lifting, it is observed that increase in the values of η slows down the velocity profile. The values of velocity profiles are taken in the interval $1.6 \leq w(r) \leq 0$.

Table 3 describes the effects of λ on the velocity profile during lifting, it is observed that increase in the values of η slows down the velocity profile.

Table 8: Effect of Br on temperature distribution $\theta(r)$, where $S_t = 0.6$, $\eta = 0.4$, $\lambda = 0.7$

r	Br = 0.2	Br = 0.4	Br = 0.6	Br = 0.8
1	3.7534307	2.6813513	1.8124572	1.7635781
1.1	3.7733108	2.6921257	1.8306481	1.7608344
1.2	3.8303437	2.7831408	1.8592126	1.7832408
1.3	3.8624387	2.7851633	1.9175208	1.8574312
1.4	3.9521792	2.7884974	1.9745186	1.8739174
1.5	3.9721452	2.8361307	2.6317534	1.9616437
1.6	3.9853713	2.8518008	2.6780063	1.9713636
1.7	3.9873402	2.8823537	2.7041501	1.9815156
1.8	3.9976241	2.9512359	2.8007186	1.9916342
1.9	3.9986452	2.9967435	2.9014631	1.9981624

Table 4 indicates the heat transfer during lifting of the fluid, it is noted that heat transfer is higher for high values of Brinkman number Br.

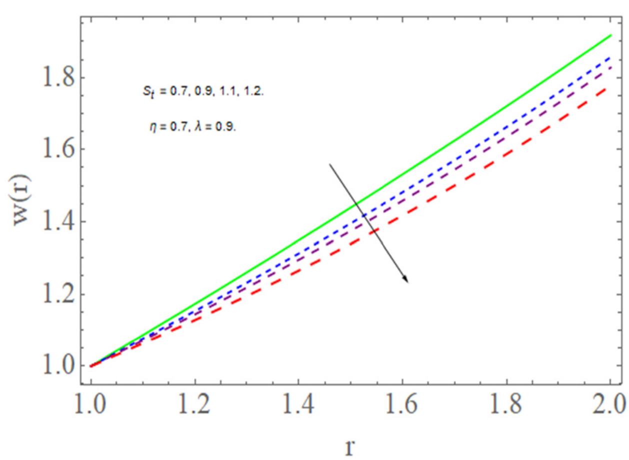

Figure 2: Influence of S_t on velocity, for lifting problem.

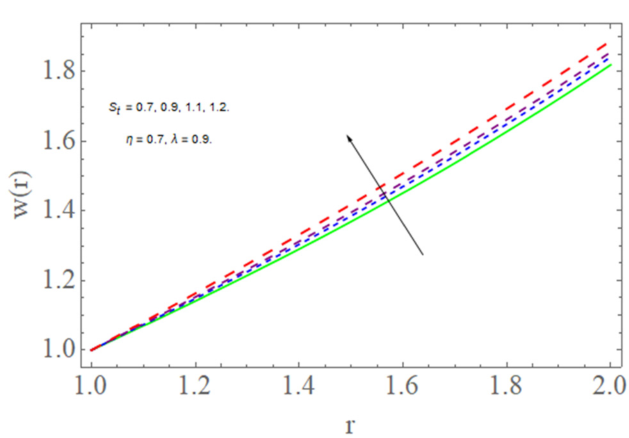

Figure 3: Influence of S_t on velocity, for drainage problem.

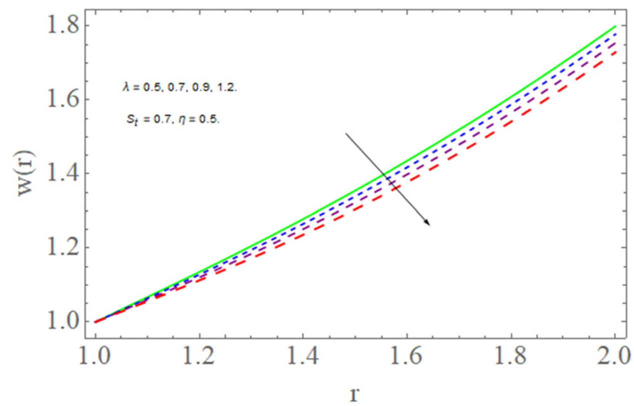

Figure 4: Impact of λ on velocity, for lifting problem.

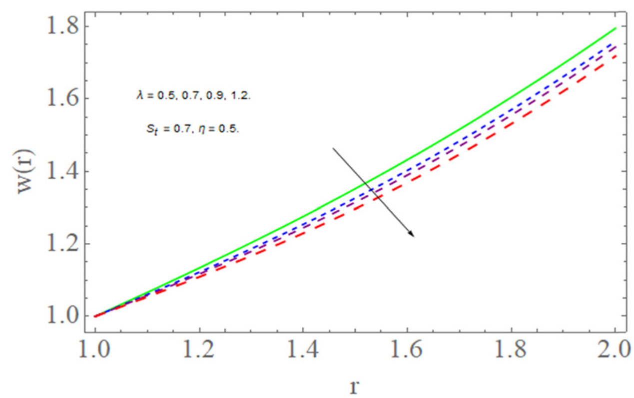

Figure 5: Impact of λ on velocity, for drainage problem.

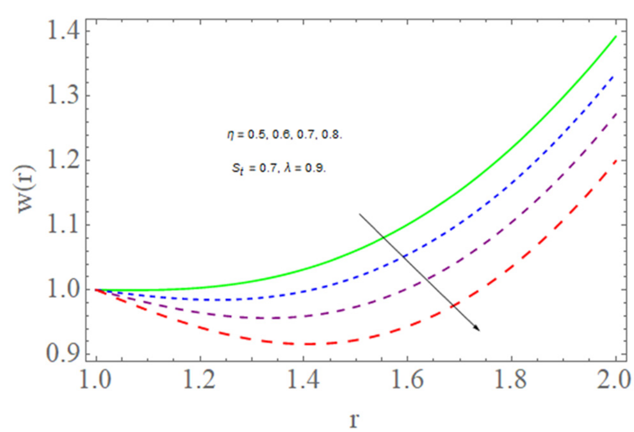

Figure 6: Impact of η on velocity, for lifting problem.

Table 5 is carried out for various values of S_t number and it is found that drainage of the fluid can be increased by increaing the Stokes number.

Table 6 depicts that drainage of the fluid slows down for higher values of η.

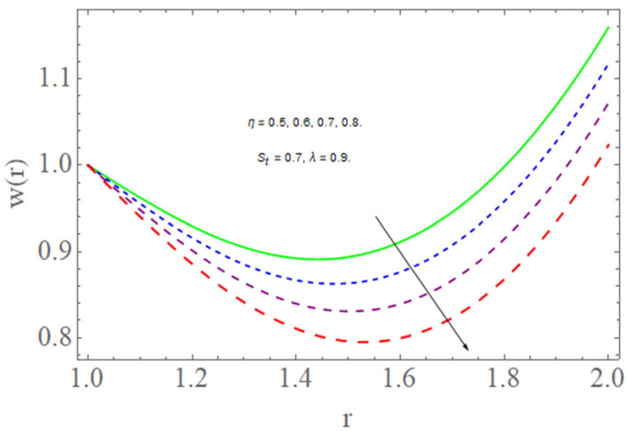

Figure 7: Influence of η on velocity, for drainage problem.

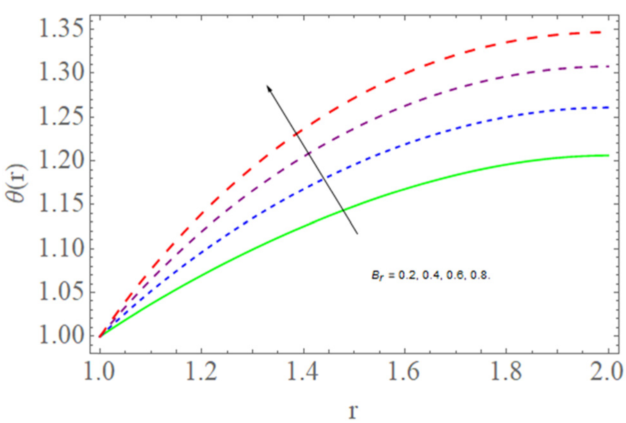

Figure 8: Effect of Br on velocity, for lifting problem.

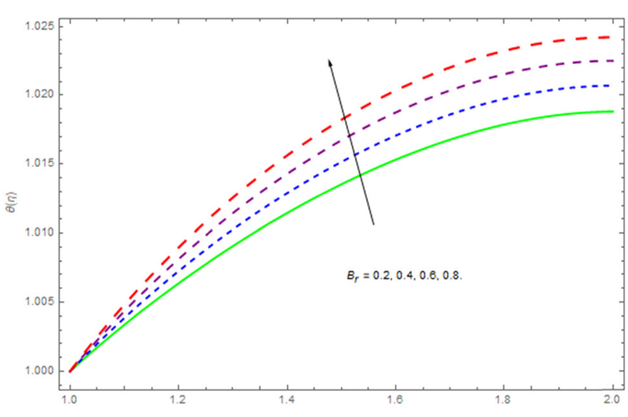

Figure 9: Impact of Br on velocity, for drainage problem.

Table 7 shows that drainage of the fluid slows down for higher values of parameter λ.

Table 8 describes that heat transfer procedure increases during drainage of the fluid with the increase in the values of Brinkman number.

6.2 Graphical description

Figures 2–9 are sketched for different values of Stokes number S_t, vorticity parameter λ, couple stress parameter η, and Brinkman number Br, considering both the cases of lifting and drainage of the fluid to note the effects of these parameters on velocity profile and temperature distribution. Figures 2 and 3 show that for increase in the values of Stokes number S_t, velocity profile slows down for lifting case and enhances for drainage case. Figures 4 and 5 are plotted for various values of vorticity parameter λ. Both the figures depict fluid share thickening behavior as velocity profile decreases for the increase in the values of λ for both lifting and drainage cases. Figures 6 and 7 are sketched for both lifting and drainage cases for different values of couple stress parameter. It is observed that like stokes number and vorticity parameter, couple stress parameter also slows down the fluid flow. Figures 8 and 9 are drawn to check the effect of Brinkman number on the temperature distribution in both lifting and drainage cases. It is observed that temperature distribution increases for both lifting and drainage cases, for higher values of Brinkman number.

7 Conclusion

The current study discusses the problem of thin film withdrawal and drainage flow of a steady incompressible, non-isothermal couple stress fluid on the outer surface of a vertical cylinder, which is modeled using the nonlinear ordinary differential equations and solved with the help of HAM, to calculate the expressions for velocity profile and temperature distribution.

The findings are as below:

- The increase in the value of vorticity parameter λ slows down the velocity field for both lifting and drainage cases.
- The increase in the values of Stokes number S_t, decreases the velocity profiles in case of lifting, while increases in case of drainage.
- The increasing values of couple stress parameter η, decrease velocity profiles for both lifting and drainage cases.
- The increasing values of Brinkman number Br increases the temperature distribution for both lifting and drainage of the fluid.

It is observed that the involved parameters have a vital role in the flow and heat transfer of the fluid.

Acknowledgment: Chutarat Tearnbucha would like to acknowledge financial support by Navamindradhiraj University through the Navamindradhiraj University Research Fund (NURF).

Funding information: The authors state no funding involved.

Author contributions: All authors have accepted responsibility for the entire content of this manuscript and approved its submission.

Conflict of interest: The authors state no conflict of interest.

References

[1] Stokes VK. Couple stresses in fluid. Phys fluids. 1966;9:1709–15.
[2] Devakar M, Sreenivasu D, Shankar B. Analytical solutions of couple stress fluid flows with slip boundary conditions. Alex Eng J. 2014 Sep 1;53(3):723–30.
[3] Jangili S, Adesanya SO, Ogunseye HA, Lebelo R. Couple stress fluid flow with variable properties: a second law analysis. Math Methods Appl Sci. 2019 Jan 15;42(1):85–98.
[4] Farooq M, Rahim MT, Islam S, Siddiqui AM. Steady Poiseuille flow and heat transfer of couple stress fluids between two parallel inclined plates with variable viscosity. J Assoc Arab Univ Basic Appl Sci. 2013 Oct 1;14(1):9–18.
[5] Naduvinamani NB, Patil SB. Numerical solution of finite modified Reynold's equation for couple stress squeeze film lubrication of porous journal bearings. Computers Struct. 2009 Nov 1;87(21–22):1287–95.
[6] Srivastava LM. Peristaltic transport of a couple stress fluid. Rheolog Acta. 1986 Nov;25(6):638–41.
[7] El Shehawey EF, Mekheimer KS. Couple stresses in peristaltic transport of fluids. J Phys D: Appl Phys. 1994 Jun 14;27(6):1163–70.
[8] Pal D, Rudraiah N, Devanathan R. A couple stress model of blood flow in the microcirculation. Bull Math Biol. 1988 Jul;50(4):329–44.
[9] Miladinova S, Lebon G, Toshev E. Thin-film flow of a power-law liquid falling down an inclined plate. J Non-Newtonian Fluid Mech. 2004 Sep 20;122(1–3):69–78.
[10] Alam MK, Rahim MT, Haroon T, Islam S, Siddiqui AM. Solution of steady thin film flow of Johnson–Segalman fluid on a vertical moving belt for lifting and drainage problems using adomian decomposition method. Appl Math Comput. 2012 Jul 1;218(21):10413–28.
[11] Shah RA, Islam S, Siddiqui AM, Haroon T. Optimal homotopy asymptotic method solution of unsteady second grade fluid in wire coating analysis. J Korean Soc Ind Appl Math. 2011;15(3):201–22.
[12] Kar M, Sahoo SN, Rath PK, Dash GC. Heat and mass transfer effects on a dissipative and radiative visco-elastic MHD flow over a stretching porous sheet. Arab J Sci Eng. 2014 May;39(5):3393–401.
[13] Nayak MK, Dash GC, Singh LP. Effect of chemical reaction on MHD flow of a visco-elastic fluid through porous medium. J Appl Anal Comput. 2014;4(4):367–81.
[14] Punith Gowda RJ, Baskonus HM, Naveen Kumar R, Prakasha DG, Prasannakumara BC. Evaluation of heat and mass transfer in ferromagnetic fluid flow over a stretching sheet with combined effects of thermophoretic particle deposition and magnetic dipole. Waves Random Complex Media. 2021 Sep 4;2021:1–9.
[15] Gul T, Islam S, Shah RA, Khan I, Shafie S. Thin film flow in MHD third grade fluid on a vertical belt with temperature dependent viscosity. PLoS One. 2014 Jun 20;9(6):e97552. doi: 10.1371/journal.pone.0097552.
[16] Ahmad S, Vieru D, Khan I, Shafie S. Unsteady magnetohydrodynamic free convection flow of a second grade fluid in a porous medium with ramped wall temperature. PLoS One. 2014 May 1;9(5):e88766. doi: 10.1371/journal.pone.0088766.
[17] Siddiqui AM, Mahmood R, Ghori QK. Homotopy perturbation method for thin film flow of a third grade fluid down an inclined plane. Chaos Solitons Fractals. 2008 Jan 1;35(1):140–7.
[18] Farooq M, Rahim MT, Islam S, Arif M. Series solutions of lifting and drainage problems of a nonisothermal modified second grade fluid using a vertical cylinder. J Appl Math. 2014 Jan 1;2014:2014–8.
[19] Farooq M, Rahim MT, Islam S, Siddiqui AM. Withdrawal and drainage of generalized second grade fluid on vertical cylinder with slip conditions. J Prime Res Math. 2013;9(1):51–64.
[20] Ahmad H, Khan TA. Variational iteration algorithm-I with an auxiliary parameter for wave-like vibration equations. J Low Frequency Noise Vib Active Control. 2019;38(3–4):1113–24.
[21] Abouelregal AE, Ahmad H, Nofal TA, Abu-Zinadah H. Thermo-viscoelastic fractional model of rotating nanobeams with variable thermal conductivity due to mechanical and thermal loads. Mod Phys Lett B. 2021 Apr 22;35:2150297.
[22] Abouelregal AE, Ahmad H, Gepreeld KA, Thounthong P. Modelling of vibrations of rotating nanoscale beams surrounded by a magnetic field and subjected to a harmonic thermal field using a state-space approach. Eur Phys J Plus. 2021 Mar;136(3):1–23.
[23] Iqbal S, Alam MF, Alimgeer KS, Atif M, Hanif A, Yaqub N, et al. Mathematical modeling and experimental analysis of the efficacy of photodynamic therapy in conjunction with photo thermal therapy and PEG-coated Au-doped TiO2 nanostructures to target MCF-7 cancerous cells. Saudi J Biol Sci. 2020;28(2):1226–32.
[24] Ali A, Islam S, Khan MR, Rasheed S, Allehiany FM, Baili J, et al. Dynamics of a fractional order Zika virus model with mutant. Alex Eng J. 2021 Nov 1;61:4821–36. doi: 10.1016/j.aej.2021.10.031.
[25] Farooq A, Kamran M, Bashir Y, Ahmad H, Shahzad A, Chu YM. On the flow of MHD generalized maxwell fluid *via* porous rectangular duct. Open Phys. 2020 Dec 17;18(1):989–1002.
[26] Li JF, Ahmad I, Ahmad H, Shah D, Chu YM, Thounthong P, et al. Numerical solution of two-term time-fractional PDE models arising in mathematical physics using local meshless method. Open Phys. 2020 Dec 23;18(1):1063–72.

[27] Ahmad H. Variational iteration method with an auxiliary parameter for solving telegraph equations. J Nonlinear Anal Appl. 2018;2(2018):223–32.

[28] Hussain A, Arshad M, Hassan A, Rehman A, Ahmad H, Baili J, et al. Heat transport investigation of engine oil based rotating nanomaterial liquid flow in the existence of partial slip effect. Case Stud Therm Eng. 2021 Oct 5;28:101500.

[29] Hussain A, Haider Q, Rehman A, Ahmad H, Baili J, Aljahdaly NH, et al. A thermal conductivity model for hybrid heat and mass transfer investigation of single and multi-wall carbon nano-tubes flow induced by a spinning body. Case Stud Therm Eng. 2021 Sep 15;28:101449. doi: 10.1016/j.csite.2021.101449.

[30] Ahmad H, Alam N, Rahim A, Alotaibi MF, Omri M. The unified technique for the nonlinear time-fractional model with the beta-derivative. Results Phys. 2021. doi: 10.1016/j.rinp.2021.104785.

[31] Asjad MI, Faridi WA, Jhangeer A, Abu-Zinadah H, Ahmad H. The fractional comparative study of the non-linear directional couplers in non-linear optics. Results Phys. 2021 Jul 4;27:104459. doi: 10.1016/j.rinp.2021.104459.

[32] Fayz-Al-Asad M, Alam MN, Ahmad H, Sarker MMA, Alsulami MD, Gepreel KA. Impact of a closed space rectangular heat source on natural convective flow through triangular cavity. Results Phys. 2021;23:104011. doi: 10.1016/j.rinp.2021.104011.

[33] Khan MN, Ahmad I, Akgül A, Ahmad H, Thounthong P. Numerical solution of time-fractional coupled Korteweg–de Vries and Klein–Gordon equations by local meshless method. Pramana. 2021 Dec;95(1):1–3.

[34] Atif M, Iqbal S, Fakhar-E-Alam M, Mansoor Q, Alimgeer KS, Fatehmulla A, et al. Manganese-doped cerium oxide nanocomposite as a therapeutic agent for MCF-7 adenocarcinoma cell line. Saudi J Biol Sci. 2020;28:1233–8.

[35] Menni Y, Ameur H, Yao SW, Amraoui MA, Lorenzini G, Ahmad H. Computational fluid dynamic simulations and heat transfer characteristic comparisons of various arc-baffled channels. Open Phys. 2021 Jan 1;19(1):51–60.

[36] Zahran EH, Bekir A, Alotaibi MF, Omri M, Ahmed H. New impressive behavior of the exact solutions to the Benjamin-Bona-Mahony-Burgers equation with dual power-law nonlinearity against its numerical solution. Results Phys. 2021;29:104730. doi: 10.1016/j.rinp.2021.104730.

[37] Mohammed WW, Ahmad H, Boulares H, Khelifi F, El-Morshedy M. Exact solutions of Hirota–Maccari system forced by multiplicative noise in the Itô sense. J Low Frequency Noise Vib Active Control. 2021;41:74–84. doi: 10.1177/14613484211028100.

[38] Hussain A, Hassan A, Mdallal QA, Ahmad H, Sherif EM, Rehman A, et al. Comsolic solution of an elliptic cylindrical compressible fluid flow. Sci Rep. 2021;11:20030. doi: 10.1038/s41598-021-99138-7.

[39] Ahmad H, Seadawy AR, Ganie AH, Rashid S, Khan TA, Abu-Zinadah H. Approximate Numerical solutions for the nonlinear dispersive shallow water waves as the Fornberg–Whitham model equations. Results Phys. 2021 Feb 16;22:103907. doi: 10.1016/j.rinp.2021.103907.

[40] Zahran EH, Mirhosseini-Alizamini SM, Shehata MS, Rezazadeh H, Ahmad H. Study on abundant explicit wave solutions of the thin-film ferro-electric materials equation. Optical Quantum Electron. 2022;54(1):1–3.

[41] Liao S. Beyond perturbation: introduction to the homotopy analysis method. CRC Press; 2003 Oct 27.